The Journal of Neuroscience, March 1995, 15(3): 1741–1754

Genetic Analysis of *Drosophila* Neurons: *Shal, Shaw,* and *Shab* Encode Most Embryonic Potassium Currents

Susan Tsunoda[1] and Lawrence Salkoff[1,2]

[1]Department of Anatomy and Neurobiology and [2]Department of Genetics, Washington University School of Medicine, St. Louis, Missouri 63110

In this study, we perform the first genetic analysis of K^+ currents in *Drosophila* embryonic neurons revealing the identity of the currents present. Unlike muscles, where the presence of *Shaker* is obvious, Shaker currents are not detectable in these neurons. In contrast, we show that *Shal* is as important in these neuronal cell bodies as *Shaker* is in muscles. Only three single-channel currents were found, all of which are genetically separable. *Shal* encodes a 4 pS transient channel. Whole-cell Shal currents have a wide variety of inactivation rates which, in contrast to a mechanism such as heteromultimer formation, is due to single Shal channels assuming different gating modes. *Shaw* encodes a 42 pS noninactivating channel distinctive for its extremely low voltage sensitivity; Shaw channels have a total equivalent gating charge of 0.90 e^- charges, in sharp contrast to 7 e^- reported for Shaker channels. An 11 pS slowly inactivating channel also present in these neurons may be encoded by the *Shab* gene. Thus, of four voltage-dependent K^+ channel genes now cloned in *Drosophila,* all except Shaker appear to be expressed in the cell bodies of these neurons. It is only in *Drosophila* that a study such as this one can be done. Because *Drosophila* contains only a single member of each of the four subfamilies of K^+ channel genes (unlike mammals), we can eliminate an entire subfamily with a mutation to a single gene. Here, we have examined the effect of eliminating each of three subfamilies. Such a task is presently impossible to accomplish in any mammalian system.

[Key words:* Drosophila, *potassium channels, mutant analysis,* Shaker, Shal, Shab, Shaw, *embryonic neurons, excitable membranes]

K^+ channels constitute perhaps the most diverse group of all ion channel families (Rudy, 1988, 1991; Hille, 1992). Not unexpectedly then, we found a wide variety of voltage-dependent K^+ currents in embryonic *Drosophila* neurons. They varied most prominently in their inactivation rates. Our goal in this study was to identify the genes encoding voltage-dependent K^+ channels expressed in these neurons, and examine how they contribute to the diversity of the whole-cell K^+ currents observed.

Mutant analysis is the simplest and most direct approach to correlate genes to the currents they encode. Since *Drosophila* contains only a single representative of each of four K^+ channel subfamilies, *Shaker, Shal, Shab,* and *Shaw,* a mutation of any one gene removes all forms of that subfamily from the entire animal. Previously, mutant analysis has been achieved only for *Shaker.* While *Shaker* mutations have been found to eliminate all of the transient A-type current in muscle (Salkoff and Wyman, 1981; Salkoff, 1983, 1985; Wu and Haugland, 1985; Solc et al., 1987; Zagotta et al., 1988; Broadie and Bate, 1993), Shaker mutations have left the majority of neuronal currents unaffected (Solc et al., 1987; Baker and Salkoff, 1990). Only in photoreceptors is *Shaker* as prominently expressed as in muscle (Hardie, 1991). Mutant analysis of the K^+ currents encoded by the three other cloned K^+ channel genes then would be of great value in identifying the K^+ currents present as well as determining whether there are currents which cannot be correlated to one of the currently cloned K^+ channel genes.

In this study, we analyzed the diversity of K^+ currents present in embryonic neurons by using *Drosophila* strains containing deficiencies of K^+ channel genes. We examined the effects of a *Shal* deficiency, a *Shaw* deficiency, and mutant alleles removing the function of the *Shaker* gene on the K^+ currents in embryonic neurons. We found that *Shal, Shaw,* and, most likely, *Shab* account for virtually all of the single-channel currents present in wild-type neurons, while *Shaker* is not present. Because it has been suggested that the *ether-a-go-go* (*eag*) gene contributes subunits to voltage-dependent K^+ channels (Zhong and Wu, 1991), we also examined these K^+ currents in eag^1 mutant neurons. The eag^1 allele has been shown to affect I_K, the delayed rectifier–type K^+ current, in *Drosophila* larval muscle. We found that none of the voltage-dependent single whole-cell currents appeared to be affected by the eag^1 mutation. We find that *Shal* encodes virtually all of the transient K^+ currents, accounting for most of the variation seen at the whole-cell level. Thus, the wide range of whole-cell currents observed in embryonic *Drosophila* neurons arises from the mix of K^+ currents generated by the *Shal, Shaw,* and *Shab* genes, and the variant currents generated by a single channel, Shal.

Materials and Methods

Cell culture. Late-gastrula cell cultures were prepared in a manner similar to previous reports (Seecof et al., 1971). Eggs were collected over

Received June 20, 1994; revised Aug. 10, 1994; accepted Aug. 16, 1994.

We thank Dr. Keith Baker for examination of macroscopic Shaw expression in *Xenopus* oocytes which suggested that Shaw channels have a low voltage sensitivity. We thank Alice Butler for performing the Northern analyses presented in this study, and Dr. Aguan Wei for Southern analyses performed to confirm that *Shal* and *Shaw* fell within the respective deficiencies used in this study. We thank Dr. Nick Tripolis for help in locating the map position of *Shal.* We also thank Dr. A. Wei, Dr. M. Saito, T. Jegla, M. Schreiber, S. Silbert, and J. Ray for helpful comments and suggestions on the manuscript. This study was supported by a grant from the National Institutes of Health, R01 NS24785-01, and a grant from the Muscular Dystrophy Association of America.

Correspondence should be addressed to Lawrence Salkoff, Department of Anatomy and Neurobiology, Washington University School of Medicine, Box 8108, 660 S. Euclid Avenue, St. Louis, MO 63110.

a 1–2 hr period and allowed to develop for about 5.5–6 hr in a humidified chamber. Eggs were rinsed with 70% ethanol, dechorionated by rolling on double-stick scotch tape, and covered with halocarbon oil. A sharp microelectrode with a broken tip was used to break through the vitelline membrane of single embryos, and all contents were removed by suction. Single embryos were dissociated into a 20 μl drop of culture medium similar to media previously described (Seecof and Donady, 1972): 18% fetal calf serum, 6 mU/ml insulin, and 1% penicillin-streptomycin (from a stock of 10 kU penicillin and 0.5 mg/ml streptomycin in 0.9% NaCl) in Schneider's Medium. Cultures were prepared on glass coverslips or Primaria (Falcon, no. 3801) tissue culture dishes. Cultures were grown at room temperature in a humidified chamber for 19–50 hr before being used for electrophysiology.

Fly stocks. Shaker stocks used were Sh^{KS133}, a missense mutation occurring between the S5 and S6 transmembrane-spanning domains (Lichtinghagen et al., 1990), and Sh^{102}, a nonsense mutation occurring between the S5 and S6 transmembrane-spanning domains (Gisselmann et al., 1989).

The *Shal* deficiency used was Df(3L)JK18; 76B1–2 to 76D5 (described in Lindsley and Zimm, 1992). *Shal* was mapped to 76B8 and confirmed to fall within this deficiency by Southern analysis (A. Wei, unpublished observations). The *Shal* deficiency was maintained over a third chromosome balancer (TM6) with a P-element insertion containing the *lacZ* gene driven by the *AbdA* (abdominal-A) promoter.

The *Shaw* deficiency used was Df(2L)edSz-1; 24A3–4 to 24D3–4 (Reuter and Szidonya, 1983; Szidonya and Reuter, 1988). *Shaw* was mapped to 24C and confirmed to fall within this deficiency by Southern analysis (Wei, unpublished observation). This deficiency was maintained over a balancer chromosome (CyO) containing the *lacZ* gene driven by the *elav* promoter (courtesy of Dr. Kalpana White).

Identifying neurons. Although whole embryos containing many different cell types are dissociated, culture conditions have been shown to favor the survival of only muscle cells and neurons (Shields and Sang, 1970; Seecof et al., 1971). We recorded from neurons which occur in clusters, reported to arise from single neuroblasts (Seecof et al., 1973). These clusters stain positive with FITC-conjugated anti-HRP (data not shown), an antibody which specifically recognizes CNS and PNS neurons in *Drosophila* (Jan and Jan, 1982). Such clusters are relatively easy to identify by morphology.

Determining the genotype of a given culture. Homozygous *Shal* and *Shaw* deficiencies cause developmental arrest in late embryogenesis. Each deficiency is maintained over a balancer chromosome containing the *lacZ* gene. The intercross of heterozygous *Shal*-deficient flies produce three different genotypes (Fig. 1): one-half heterozygous, one-quarter homozygous for the balancer chromosome, and one-quarter homozygous *Shal* deficiency. Cells homozygous and heterozygous for a balancer chromosome will synthesize β-galactosidase and stain blue when treated with X-gal. Only embryos homozygous for the deficiency will not stain.

Fixing and staining cultures. After recording, cells were immediately fixed for 3–5 min in 2% formaldehyde (from a 37% stock solution) and 0.4% glutaraldehyde (from a 25% stock solution) in phosphate buffer solution (PBS). Cultures were rinsed with PBS after fixing and stained overnight at 30°C with an X-gal solution containing 1 mg/ml X-gal (from an 8% stock made up in DMSO), 16 mM K-ferrocyanide, 16 mM K-ferricyanide, and 2 mM $MgCl_2$ in PBS, pH 7.2–7.3. Cultures were rinsed with PBS and checked for blue staining.

Electrophysiology. The patch-clamp technique was used to record whole-cell currents and single-channel currents from outside-out patches (Hamill et al., 1981). Electrodes were pulled using borosilicate glass and had resistances between 6 and 12 MΩ for whole-cell currents. Whole-cell currents averaged about 320 pA at +20 mV, and series resistance was not compensated for; with a series resistance of about 30 MΩ, the voltage error would be 10 mV. Since inactivation rates of transient currents were relatively voltage independent, we would not expect that this error would have an effect on our measurements. In addition, most whole-cell results were confirmed at the single-channel level. Borosilicate glass electrodes were used for single-channel recording from outside-out patches, coated with Sylgard, and fire polished; resistances in solutions used ranged from 25 to 50 MΩ. To avoid the cells detaching from the dish and thus adhering to the electrode when patches were pulled, special care was taken to fire polish pipettes such that only a small amount of the glass surface would make contact with the cell membrane. In this way, the success rate of pulling outside out patches was fairly high (about 75%).

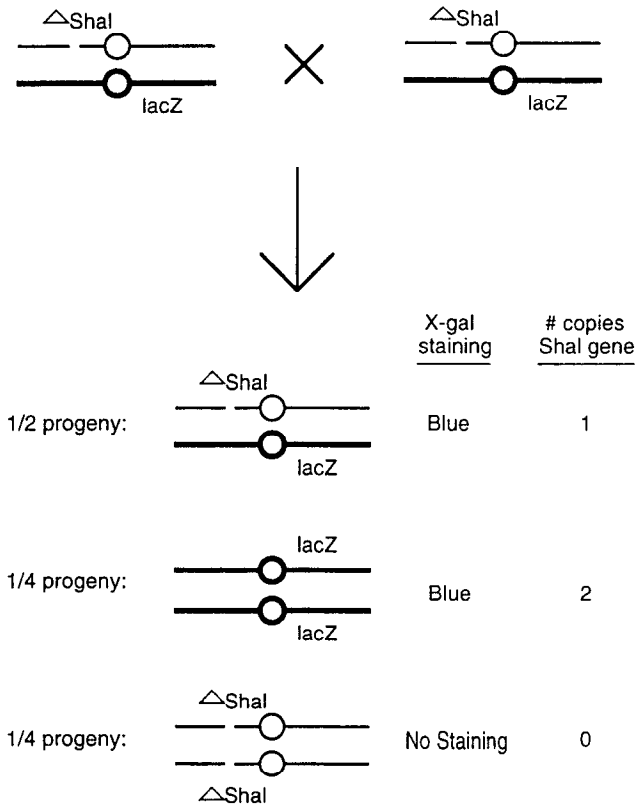

Figure 1. Genetic cross used to identify homozygous *Shal* (or *Shaw*)-deficient embryos. Parent stock: *Shal* deficiency (Df[3L]JK18/[TM6, P(w+, *AbdA-lacZ*)]). Balancer has an inserted P-element containing the *lacZ* gene driven by the *Abdominal-A* promoter. *Shal*-deficient third chromosomes are represented by a *thinner line*; TM6, represented by *thicker lines,* is a balancer for the third chromosome and contains the *lacZ* gene. Cells from embryos containing at least one copy of the *Shal* gene will stain blue with X-gal treatment; cells from embryos which are deficient for the *Shal* gene will not stain blue.

Data was acquired using an Axopatch-1B or 200A amplifier (Axon Instruments). Data acquisition software used was CCURRENT (Dr. Keith Baker; Indec, Sunnyvale, CA). Analysis software included CQUANT (Dr. Keith Baker), VPROC (Dr. Christopher Lingle), and QUATTRO PRO.

Where indicated, the number of channels in a patch was determined by imposing voltage steps under which the channel(s) had a relatively high probability of opening, and looking for simultaneous openings of multiple channels. This number is thus a lower limit of the number of channels present, and probably an underestimate in the case of Shaw channels, which have a low open probability

Solutions were as follows (in mM): internal, 140 KCl, 2 $MgCl_2$, 11 EGTA, and 10 HEPES; external, 140 NaCl, 2 KCl, 6 $MgCl_2$, 5 HEPES, 20–35 sucrose, and 100 nM tetrodotoxin. Solutions used for single-channel recording often contained aspartate as the major anion instead of chloride.

Expression in Xenopus *oocytes.* cRNA was prepared and injected into *Xenopus* oocytes as previously described (Wei et al., 1990). Outside-out patches were pulled from oocytes 2–5 d after injection. Solutions and data acquisition and analysis software were as described above, except for the substitution of 4 mM $MgCl_2$ plus 2 mM $CaCl_2$ for 6 mM $MgCl_2$.

Statistics. Sixty-four out of 86 patches (74%) from neurons containing a *Shal* gene were observed to contain at least one of the 4 pS channels. The $100(1 - a)$% confidence interval for such a population proportion, p, based on N independent observations is given by

$$(p - [z_b\,(p * q/N)^{1/2}],\ p + [z_b\,(p * q/N)^{1/2}]),$$

where p = the proportion of patches containing a Shal channel in N wild-type patches ($p = 0.7442$ in this case), $b = a/2$, $q = 1 - p$, and

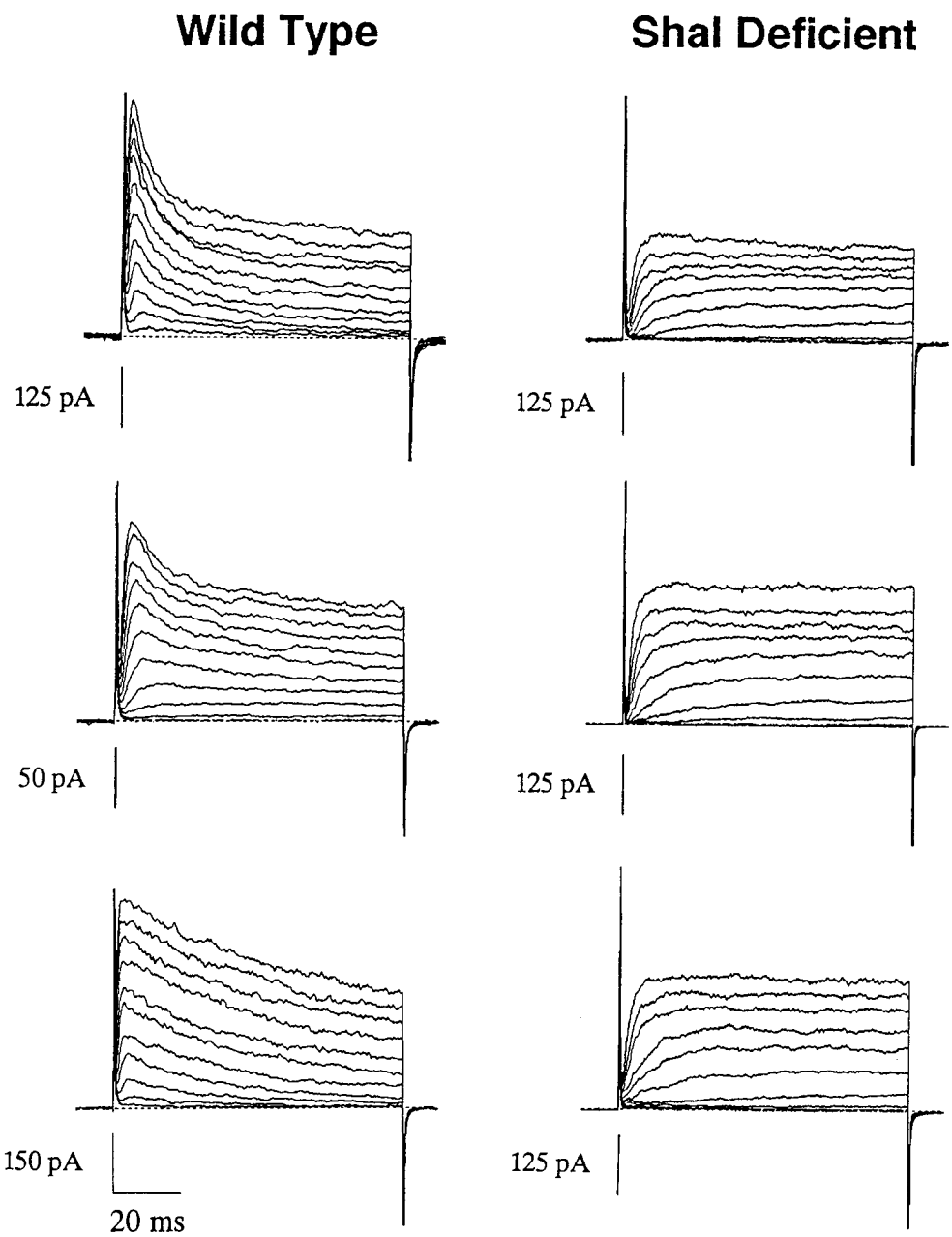

Figure 2. A *Shal* genetic deficiency removes transient K^+ currents from embryonic *Drosophila* neurons. *Left column,* Whole-cell recordings from three representative wild-type neurons. Rates of inactivation of transient components varied from cell to cell. *Right column,* Whole-cell recordings from three representative *Shal*-deficient neurons which typically contain only slowly inactivating and noninactivating currents. Voltage jumps were from −50 mV to +50 mV in 10 mV increments from a holding potential of −90 mV. Cell capacitances ranged from 1.22 pF to 3.26 pF, averaging 2.39 pF.

z_b is the critical value for standard normal curves (Devore, 1982). Thus the 95% confidence interval ($a = 0.05$, $b = 0.025$, $z_b = 1.645$) for the proportion of patches containing at least one of the 4 pS channels is 0.7442 ± 0.077. Therefore, from 20 patches from *Shal*-deficient neurons, we would expect 13–17 of them to contain a 4 pS channel within a 95% confidence interval. The probability that none of the 20 would contain a single 4 pS channel is less than $2.78 * 10^{-10}$. Since the 4 pS channel was never observed in these *Shal*-deficient neurons, we conclude that this channel is encoded by the *Shal* gene.

Of 88 patches from neurons containing the *Shaw* gene, 49 contained at least one 42 pS channel, giving us a proportion of 0.5568. By similar calculations to those described for *Shal,* the 95% confidence interval is 0.5568 ± 0.053. Therefore, out of the 31 patches pulled from *Shaw*-deficient neurons, we would expect, within this 95% confidence interval, that 15–19 of them would have contained a 42 pS channel. The probability that none of the 31 would contain a single 42 pS channel is less than $3.68 * 10^{-10}$. Since this 42 pS channel was never observed in *Shaw*-deficient neurons, we conclude that it is encoded by the *Shaw* gene.

Results

Wide range of K^+ currents in embryonic neurons

To determine which genes are responsible for the total repertoire of K^+ currents in embryonic neurons, we began by examining the types of currents present in wild-type neurons. We later separated these currents using deficiencies of particular K^+ channel genes. A survey of whole-cell K^+ currents from a large number of wild-type neurons might have enabled us to place all currents into a small number of categories based on properties such as their inactivation rates. However, we found this to be impossible because whole-cell K^+ currents varied in a graded manner, from cell to cell, especially in their inactivation rates. Figure 2 shows some examples of the variation seen in embryonic neurons.

Whole-cell currents varied over several orders of magnitude in their rates of inactivation. Most (95%) wild-type neurons (*N*

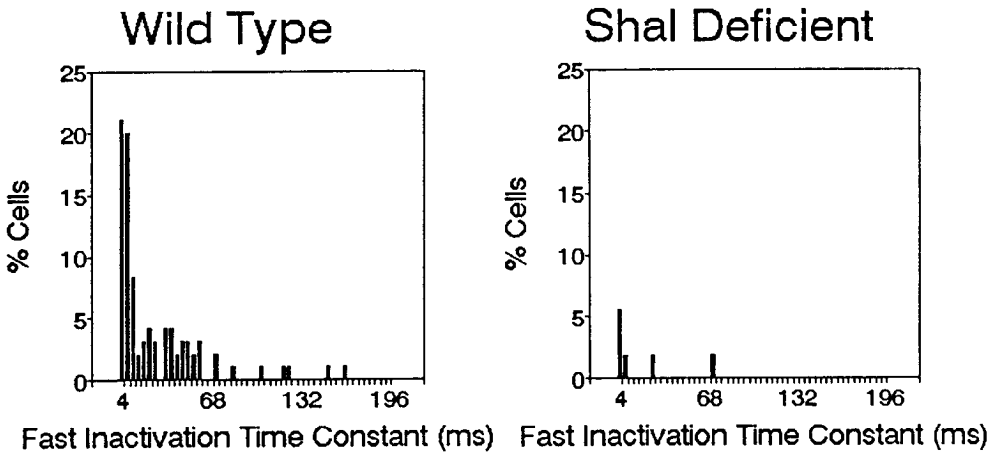

Figure 3. Distribution of fast inactivation time constants in wild-type and *Shal*-deficient neurons. *Left,* Histogram of fast inactivation time constants of transient currents present in wild-type neurons (N = 95). *Right,* Histogram of fast inactivation time constants of transient currents present in neurons deficient for the *Shal* gene (N = 54).

= 95) contained a transient component, as defined by a fast inactivation time constant less than 200 msec (at +20 mV). Transient current components were usually accompanied by a slowly inactivating component; the transient component made up 38–100% of the total whole-cell current, averaging about 77% (N = 79). The distribution of fast inactivation time constants ranged from 1 to 163 msec (N = 82) (Fig. 3). A notable characteristic of the whole-cell transient currents was the relative voltage-independence of their inactivation time constants. Interestingly, this characteristic is typical of Shal currents (Pak et al., 1991), but quite unlike Shaker currents which have faster inactivation rates at more positive voltages (Zagotta and Aldrich, 1990).

Another property which showed variation was steady-state inactivation. Steady-state inactivation data was usually fit best by a double Boltzmann function, indicating two separable components. These two functions corresponded to a transient and a slowly inactivating component (Fig. 4). Transient currents always corresponded to the more hyperpolarized component, which enabled us to separate transient currents from slowly inactivating currents. Slowly inactivating currents were isolated by inactivating the transient component with a depolarizing prepulse (Fig. 4*C*). Transient currents were isolated by subtracting slowly inactivating currents from the total whole-cell current (Fig. 4*C*). Transient currents had an average steady-state inactivation midpoint ($V_{1/2}$) of −72 mV. This steady-state inactivation profile is also more characteristic of Shal than Shaker currents when expressed in the *Xenopus* oocyte expression system, where Shaker had a $V_{1/2}$ of −35 mV and Shal had a $V_{1/2}$ of −62 mV (Wei et al., 1990).

The Shal gene encodes virtually all transient K⁺ channels, and is responsible for most of the variability

With the great variety of K⁺ currents present in embryonic neurons, it was unclear whether a deficiency of any single K⁺ channel gene would be detectable. We suspected, however, that *Shal* might account for at least a portion of the transient current in these neurons because of its resemblance to Shal currents in *Xenopus* oocyte expression studies, and Northern analysis suggesting that *Shal,* and not Shaker, is prominently expressed in the late embryo (see Fig. 11). To test this hypothesis, we used a genetic deficiency of the *Shal* locus that would eliminate all Shal currents, including those resulting from alternatively spliced forms of the gene. We compared whole-cell current recordings from wild-type neurons to those of *Shal*-deficient neurons, and identified the current(s) removed by the deficiency. Surprisingly, most transient currents were absent in *Shal*-deficient neurons. While transient K⁺ currents were seen in 95% of wild-type neurons (N = 95), only 13% of neurons deficient for the *Shal* gene contained a transient current (N = 54); typically, only a slowly or noninactivating whole-cell current, uniform in appearance, remained (Fig. 2). Wild-type transient currents eliminated by the *Shal* deficiency had a wide range of fast inactivation time constants (Fig. 3). The *Shal* gene might generate channels with such a broad range of inactivation rates by several mechanisms including alternative RNA splicing, as well as heteromultimerization of these different forms. Further investigation into the mechanism underlying the variability observed required us to move to the single-channel level.

Shal encodes a 4 pS channel

We investigated the properties of single-channel currents expressed by the *Shal* gene by examining those single-channel currents in wild-type cells which were eliminated by the *Shal* deficiency. This study was feasible because only three distinct voltage-dependent K⁺ channels were detected in outside-out patches from wild-type neurons (Table 1): (1) a 4 pS rapidly inactivating channel; (2) a 42 pS noninactivating channel; and (3) an 11 pS slowly inactivating channel. The smallest of the three channels observed (4 pS) was identified as the Shal channel because neurons from *Shal*-deficient embryos (N = 20) never contained channels of this conductance, while Shal channels were observed in 74% of patches from neurons containing at least one copy of the *Shal* gene (N = 86). The 4 pS channel was also seen at a similar frequency in neurons mutant for the *Shaker* gene or deficient for the *Shaw* gene (Table 1), showing that the *Shaker* and *Shaw* genes do not contribute subunits to the 4 pS channel. Figure 5 shows the current–voltage relation of these channels; a line fit by linear regression through these points yields a slope conductance of 3.9 pS.

Besides their small size, a second characteristic property of Shal channels is their hyperpolarized voltage operating range. Figure 5 shows the steady-state inactivation profile of ensemble-averaged Shal currents from a single patch containing approximately seven Shal channels. Shal channel activity in this patch was half-inactivated with a prepulse to −105 mV, and completely inactivated with a prepulse to −75 mV. This extremely hyperpolarized steady-state inactivation curve was typical among Shal channels in outside-out patches, but approximately 30 mV more hyperpolarized than whole-cell Shal currents observed ei-

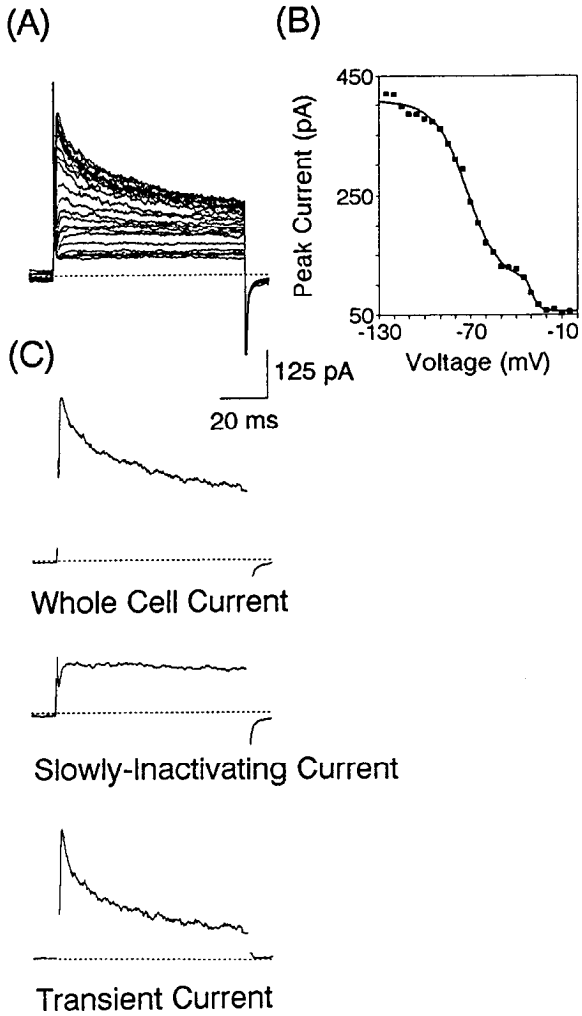

Figure 4. Separation of transient currents from slowly inactivating currents. *A*, Example of whole-cell currents during a steady-state inactivation voltage paradigm. Test voltage jumps were at +50 mV. Each test jump was preceded by a 500 msec prepulse to potentials from −125 to −5 mV, in 5 mV increments. *B*, Steady-state inactivation curve from the same cell; peak current is plotted versus prepulse potential. Data points are fit with the sum of two Boltzmann equations: $I = I_{max}/(1 + \exp[(V - V_{1/2})/k])$. Transient component is represented by the first Boltzmann with the following parameters: I_{max} = 300.26 pA, $V_{1/2}$ = −72.1 mV, k = 10.58 mV/*e*-fold shift; slowly inactivating component is represented by the second Boltzmann with the following parameters: I_{max} = 51.29 pA, $V_{1/2}$ = −29.5 mV, k = 2.18 mV/*e*-fold shift. Transient current components had a $V_{1/2}$ averaging −72.03 mV (±12.32) with a slope factor of 8.67 (±3.58) mV/*e*-fold shift (N = 79). In contrast, slowly inactivating currents had an average $V_{1/2}$ of −36.97 mV (±10.17) with a slope factor of 4.00 (±2.35) mV/*e*-fold shift (N = 51). *C*, Whole-cell current, from *A*, with a prepulse to −125 mV. Slowly inactivating current, from *A*, with a prepulse to −45 mV which completely inactivates the transient component, leaving only the slowly inactivating component as shown. Transient current, transient component revealed by subtracting the slowly inactivating current from the total whole-cell current. Capacitative artifact is partially clipped in each trace.

ther in neurons or in the *Xenopus* oocyte expression system. We cannot currently account for this difference. However, similar discrepancies between the voltage dependence of whole cell and patch recordings have been reported previously for Shaker channels in *Drosophila* photoreceptors (Hardie, 1991) and for Na^+ channels in bovine chromaffin cells (Fenwick et al., 1982). Nevertheless, we feel that these 4 pS channels do represent the conductance that carries the whole cell transient current because the deficiency of *Shal* removes both these transient single channels and the transient whole cell current. As with whole-cell transient currents, Shal ensemble-averaged currents showed an apparently voltage-independent inactivation rate.

Table 1. Frequency of single channels observed in different genotypes

Single channels observed in membrane patches	Genotype of neuronal patches			
	Wild type	*Shal* deficient	*Shaw* deficient	*Shaker*
Shal				
4 pS	33/44	**0/20**	15/22	16/20
rapidly inactivating	(75%)	**(0%)**	(68%)	(80%)
Shaw				
41 pS	31/53	8/15	**0/31**	10/20
noninactivating	(58%)	(53%)	**(0%)**	(50%)
Shab-like				
11 pS	8/49	3/13	2/27	2/29
slowly inactivating	(16%)	(23%)	(7%)	(7%)

The number of patches in each column is variable because separate studies were sometimes done in which special attention was paid to a particular channel type requiring special conditions. For example, only patches with a very low noise level were used for the detection of Shal channels. Most patches contained between one and four channels. A few patches were eliminated because too many channels were present. All channels appeared to be randomly distributed.

Single Shal channels have different gating modes with different inactivation rates

As with transient whole-cell currents, inactivation rates of ensemble-averaged currents of Shal channel activity varied among patches from different cells. Inactivation was usually fit best by a double exponential function (Fig. 6). Ensemble-averaged Shal currents displayed a range and distribution of fast inactivation time constants (Fig. 6) similar to whole-cell wild-type transient currents (Fig. 3, left). Thus, in both the excised patch and whole-cell configurations, Shal currents have variable inactivation rates extending over a similar range. Since excised patches containing small numbers of Shal channels exhibited markedly different inactivation rates, we surmised that single Shal channels must also behave in a markedly varied fashion. To explore this, we examined patches containing only single Shal channels, and found that they also display variable inactivation rates similar in range and distribution (Fig. 6) to patches containing multiple Shal channels (Fig. 6), as well as whole-cell transient (Shal) currents.

One explanation for Shal channel variability might be alternative RNA splicing. However, this is unlikely due to an observation of an apparently single neuronal Shal channel spontaneously switching gating behavior from one mode to another. The first mode gave rise to an ensemble-averaged current with a very fast inactivation rate; the second gave rise to a current with a much slower inactivation rate. Figure 7*A* shows these currents before (left) and after (right) the change in gating modes. The fast gating mode was characterized by short bursts of channel openings at the onset of a voltage jump, which produced a very rapidly inactivating component. This was followed by a sustained component, due to frequent reopenings of the channel (Fig. 7*A*, left). In contrast, the slower gating mode produced a

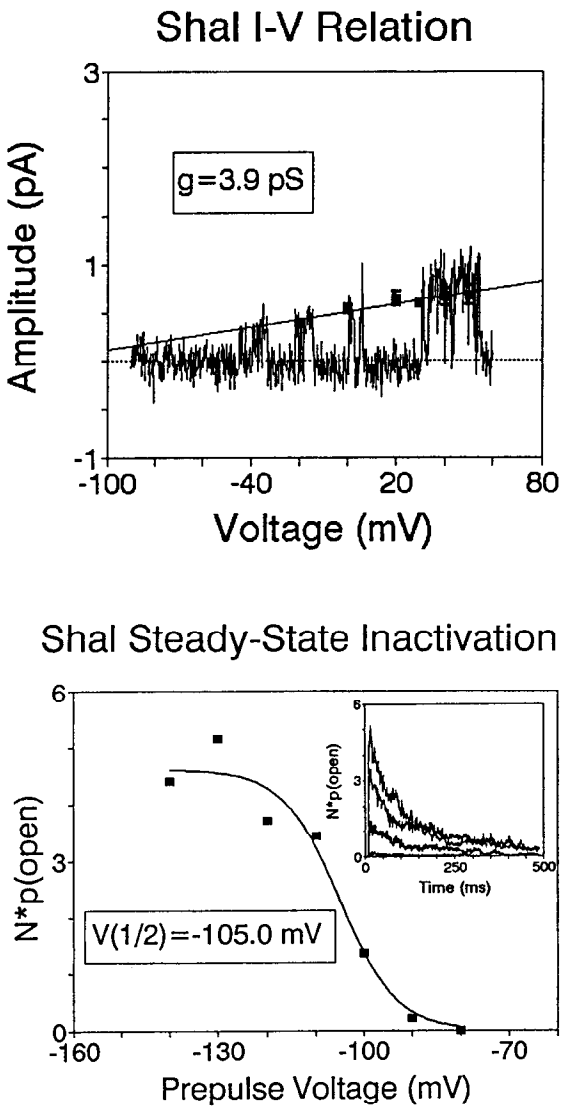

Figure 5. *Shal* expresses a 4 pS rapidly inactivating channel with a hyperpolarized steady-state inactivation curve. *Top,* Single-channel current amplitude versus voltage. Data points (■) represent average single-channel amplitudes from four to eight patches. Standard deviations are as indicated. A line fit by linear regression to these points predicts a slope conductance of 3.9 pS. Amplitudes were determined by fitting amplitude histograms with a Gaussian distribution. Asymmetrical K^+ solutions were used (see Materials and Methods). Superimposed on this graph is a single record of Shal channel activity while the voltage was ramped from −80 to +60 mV. Data used for amplitude histograms was digitized at 0.195 msec/point and filtered at 2 kHz. Ramp record was digitized at .488 ms/point. *Bottom,* Steady-state inactivation curve of Shal channels in an outside-out patch containing approximately seven channels. Data points represent peak ensemble-averaged $N * p(\text{open})$, where N = number of channels, plotted versus prepulse potential. Data points are fit with a Boltzmann equation, $I = I_{max}/(1 + \exp[(V - V_{1/2})/k])$; I_{max} = 4.62, k = 5.86 mV/e-fold shift, $V_{1/2}$ = −105.01 mV. *Inset,* Ensemble-averaged currents of Shal channel activity during voltage jumps to a test potential of +20 mV. Each ensemble-averaged current was constructed from voltage jumps (19–25 sweeps) which were preceded by a prepulse to (in order from *top* to *bottom*) −130, −110, −100, and −90 mV. Data were digitized at 0.488 msec/point and filtered at 2 kHz.

more slowly inactivating ensemble-averaged current, due to longer bursts of channel openings at the onset of a voltage jump. In this mode, the channel ultimately entered an absorbing inactivated state. Thus, the single Shal channel gave rise to ensemble-averaged currents with inactivation rates that virtually spanned the range of transient macroscopic currents recorded in wild-type neurons.

Regardless of whether single channels often change gating modes, most single Shal channels (N = 11) can be categorized as being in either a fast or slow gating mode. Figure *7B* shows two such examples: one channel in a fast gating mode, another in a slow gating mode. Hence, the variable inactivation rates of whole-cell transient currents could be due to different proportions of Shal channels in either a fast or slow gating mode. Modulation of Shal channels by a process such as phosphorylation may play a role in determining the gating mode in which a channel resides.

In order to investigate whether Shal channels exhibit variable inactivation rates in their normal cellular environment, we also examined Shal channels in cell-attached patches. In this mode, we observed Shal channels in both the fast and slow gating modes described (data not shown). Thus, this variability does not appear to be an artifact due to patch excision into artificial solutions.

Delayed rectifier–type currents present in Shal-deficient neurons: evidence for Shaw and Shab

After determining that *Shal* was responsible for transient currents, we investigated the genes responsible for the delayed rectifier–type currents (DR currents) remaining in *Shal*-deficient neurons. The Shaw and Shab K^+ channels were candidates for some of these non-Shal currents because they carry similar DR currents when expressed in *Xenopus* oocytes (Wei et al., 1989). Northern analysis also suggested that both genes are expressed in the late embryo (see Fig. 11). DR currents in neurons sometimes had a noninactivating component, similar to Shaw (Wei et al., 1989), and a slowly inactivating component similar to Shab (Pak et al., 1991).

Shaw channels were first expressed in *Xenopus* oocytes to observe single-channel properties which might aid in identifying Shaw channels in embryonic neurons. We found that Shaw channels have several distinctive properties, including an unusually low voltage sensitivity, brief open times, and a large conductance (>40 pS). A similar channel was then identified in wild-type *Drosophila* neurons (Fig. 8). Of the three types of single channels observed in embryonic neurons, this 42 pS channel was the largest. To verify that this channel was, indeed, encoded by *Shaw,* we investigated whether a genetic deficiency of *Shaw* would eliminate it. The 42 pS channel was detected in 56% of patches from neurons having a wild-type *Shaw* gene (N = 88) (Table 1), but never observed in patches from *Shaw*-deficient neurons (N = 31). Shaw channels were also detected in *Shal*-deficient and *Shaker* mutant neurons at a frequency similar to wild type (Table 1), showing that *Shal* and *Shaker* do not contribute subunits to the 42 pS channel. Hence, we conclude that the *Shaw* gene does encode this 42 pS channel.

Shaw channels have an extremely low voltage sensitivity

In working with Shaw channels, we noted that their open probability remained low even at very positive voltages, giving the impression of a channel that is very weakly responsive to voltage. To confirm this impression, open probability of Shaw chan-

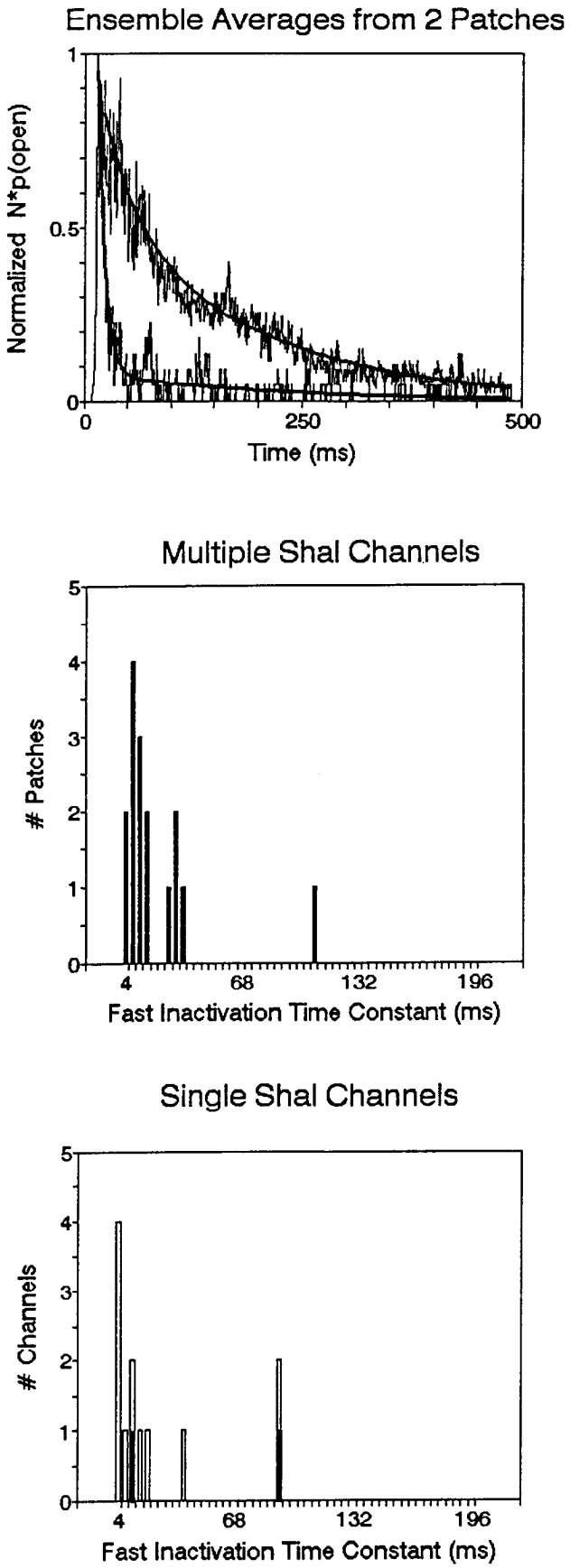

Figure 6. Shal channels in different cells have different inactivation rates. *Top,* Shal ensemble-averaged currents from patches pulled from two different cells showing different rates of inactivation; peak current nels in neurons was plotted versus voltage (Fig. 9). Data points were fit with a Boltzmann equation to the fourth power, consistent with the same model of four closed-state transitions before opening (Zagotta and Aldrich, 1990), as assumed for macroscopic data analysis. A total equivalent gating charge for opening a single channel was determined from this fit to be 0.90 ($\pm$0.070) e^- charges (N = 3). This value is similar to 0.86 e^- obtained for macroscopic Shaw currents expressed in *Xenopus* oocytes (Baker, 1992). The voltage sensitivity of Shaw channels is so low that, although they are reported to begin opening between −80 and −70 mV (Wei et al., 1990), by extrapolation of their activation curve (Fig. 9), they would not reach a p(open) of 0.95 until 558 mV.

To determine the total equivalent gating charge for Shaw channels in a model-independent manner, we examined the semilogarithmic plots of open probability versus membrane voltage (Fig. 9). From the limiting slopes of these plots, we could determine the lower limit estimate of the total equivalent gating charge needed to move through the membrane to open a single channel (Almers, 1978). We calculated this lower limit of equivalent gating charge to be 0.54 ($\pm$0.086) e^- charges (N = 3). Previous reports showed that Shaker channels have an equivalent gating charge of 6 e charges determined by similar calculations (Logothetis et al., 1992). Thus, calculated in both a model-dependent and model-independent manner, the total equivalent gating charge of Shaw channels is extremely low.

In addition to its low voltage sensitivity, Shaw channels have a very short mean open time of about 1 msec. Open time histograms were best fit with a single exponential (data not shown) and were voltage independent. This short mean open time contributes to the low open probability of Shaw channels and is unusual for a delayed rectifier–type current. Shaw channels in cell-attached patches appeared to behave similarly to those in excised outside-out patches, exhibiting the same unusual properties described above (data not shown). Shaw channels showed no sign of inactivation even at depolarized potentials and were completely blocked by 5 mM 4-aminopyridine (data not shown). All of these properties were common to Shaw channels in embryonic neurons and Shaw channels expressed in the *Xenopus* oocyte expression system.

←

of each was normalized and aligned for direct comparison of inactivation rates. Currents were fit with the double exponential function: $N * p(\text{open}) = A * \exp[-t/T(fast)] + B * \exp[-t/T(\text{slow})]$; N = number of channels observed to be in a given patch, p(open) = probability of a single channel being open. *Top trace,* Slower ensemble-averaged current with T(fast) = 37.12 msec; *bottom trace,* faster ensemble-averaged current with T(fast) = 8.12 msec. Patches contained three and two Shal channels, respectively, and ensemble averages were constructed from 85 and 89 sweeps, respectively. Voltage jumps were to a test potential of 0 mV; a 500 msec prepulse to −120 mV preceded each voltage jump. *Middle,* Histogram of fast inactivation time constants from patches containing multiple Shal channels (N = 16 patches). Ensemble averages were constructed from Shal channel activity during voltage jumps to +20 mV, 480 msec in duration. Ensemble averages were fit with a double exponential function, as in *A*. X-axis represents fast inactivation time constants binned every 4 msec; y-axis represents the number of patches. *Bottom,* Histogram of fast inactivation time constants from patches containing a single Shal channel (N = 11 patches). Ensemble averages were constructed and fit as described in *B*. Y-axis represents the number of channels displaying a particular fast inactivation time constant. *Solid bars* indicate single channel that switched gating modes (Fig. 7*A*). All data were digitized at 0.488 msec/point and filtered at 2 kHz.

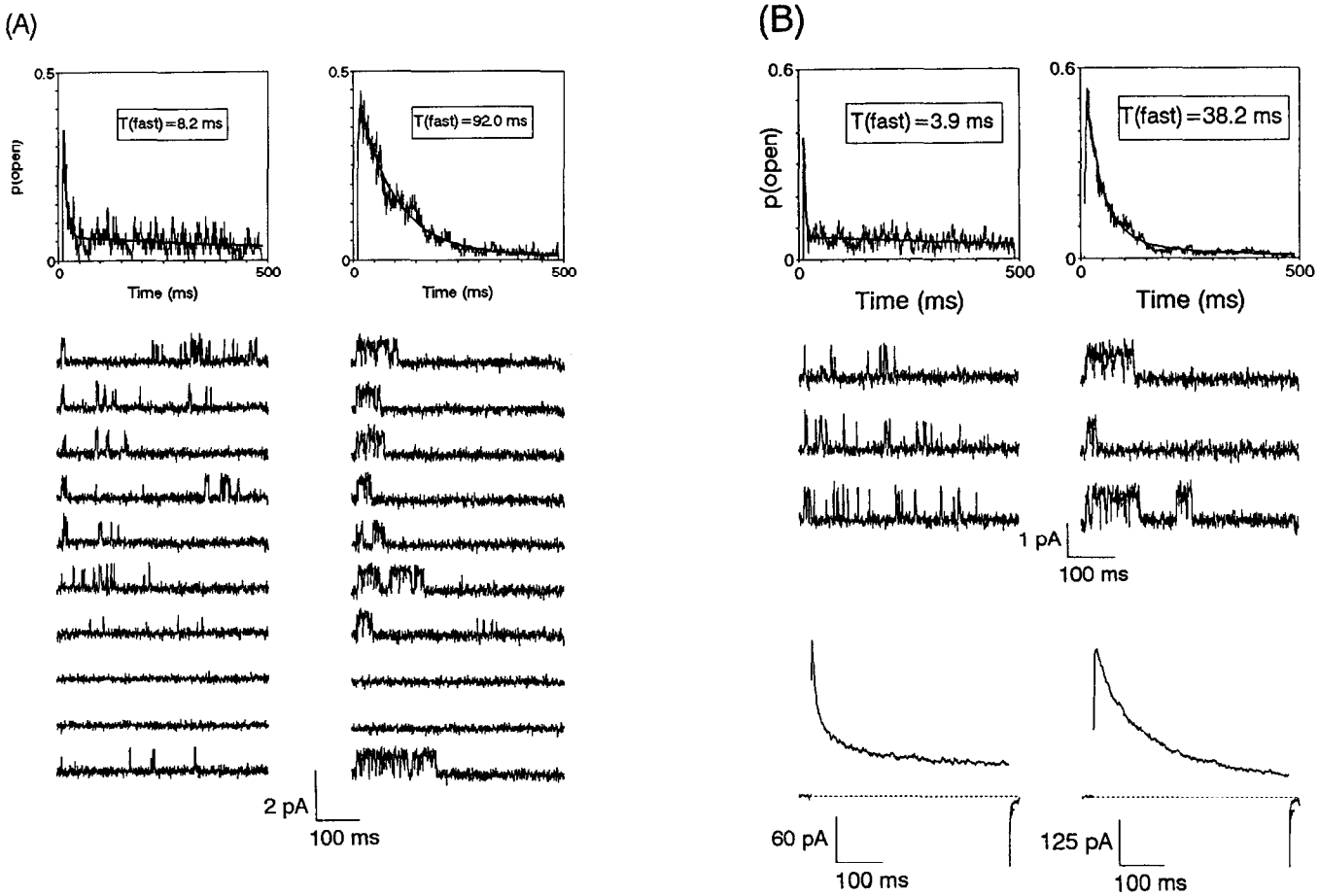

Figure 7. Shal channels switch gating modes. *A*, A single Shal channel switches from a fast gating mode (*left*) to a slower gating mode (*right*). Ten consecutive voltage jumps to +20 mV are shown below for each mode. Ensemble averages were constructed from 71 sweeps (*left*) and 110 sweeps (*right*). Membrane was prepulsed for 500 msec to −130 mV before each voltage jump. Double exponential fits are shown, where $p(\text{open}) = A * \exp(-t/T[\text{fast}]) + B * \exp(-t/T[\text{slow}])$. *Left*, $T(\text{fast}) = 8.2$ msec, $A = 1.18$, $T(\text{slow}) = 928.25$ msec, $B = 0.06$. *Right*, $T(\text{fast}) = 92.01$ msec, $A = 0.471$, $T(\text{slow}) = 6.47 * 10^{19}$, $B = 9.21 * 10^{-3}$. *B*, Two other patches each containing only a single Shal channel; each appears to be stable in one of the two gating modes seen in *A*. Three records showing single-channel activity from each patch are shown below ensemble averages. Ensemble averages were each constructed from 150 voltage jumps to +20 mV. For comparison, examples of two whole-cell transient currents which inactivate at rates similar to ensemble-averaged currents are shown below for comparison. Cells were held at −90 mV and test pulses were to +20 mV. Capacitative transients were partially removed. All single-channel data was digitized at 0.488 msec/point and filtered at 2 kHz.

Shab-like channels

Because they have no inactivation, Shaw channels cannot account for all of the DR currents in embryonic neurons; the most prominent macroscopic current present in *Shal*-deficient neurons is a slowly inactivating current. Although a genetic deficiency of the *Shab* gene was not available, we nevertheless suggest that the *Shab* gene (or a very similar gene) encodes the remaining slowly inactivating current. This is based on similarities between neuronal Shab-like currents and *Drosophila* Shab currents expressed in *Xenopus* oocytes. Of the three single-channel currents observed in neurons, only the 11 pS channel can account for this slowly inactivating current. Ensemble-averaged currents from the 11 pS channel were slowly inactivating and closely matched ensemble-averages from Shab channels expressed in *Xenopus* oocytes (Fig. 10). In both cases, this was due to similar long bursts of channel openings followed by quiescent periods (Fig. 10). Activation kinetics of neuronal Shab-like channels and *Drosophila* Shab channels expressed in *Xenopus* oocytes were also similar. Figure 10 shows that ensemble-averaged currents from both reached peak current in 27 msec at 0 mV. Another behavior common to both was an apparent "rundown" of single-channel currents; currents were often seen when patches were just excised but disappeared after a few minutes, rarely reappearing. This behavior was common with Shab-like channels but rarely seen with Shal or Shaw channels. "Rundown" probably accounts for the relatively low frequency (13% of patches, $N = 118$) at which Shab-like channels were observed in neurons, since inactive channels may have been present in a higher percentage of patches. Neuronal Shab-like channels had a conductance of 11 pS, as compared with 18 pS for Shab channels observed in the *Xenopus* oocyte expression system (Fig. 10). At the whole-cell level, slowly inactivating currents remaining in *Shal*-deficient neurons have an average steady-state inactivation midpoint of −37 mV, comparable to −46 mV for *Drosophila* Shab channels expressed in *Xenopus* oocytes (Pak et al., 1991).

We also observed Shab-like channels in *Shal*-deficient, *Shaw*-deficient, and *Shaker* mutant neurons (Table 1), which eliminates those K^+ channel genes as possible contributors to the Shab-like channels. Northern analysis showed that *Shab* is prominently

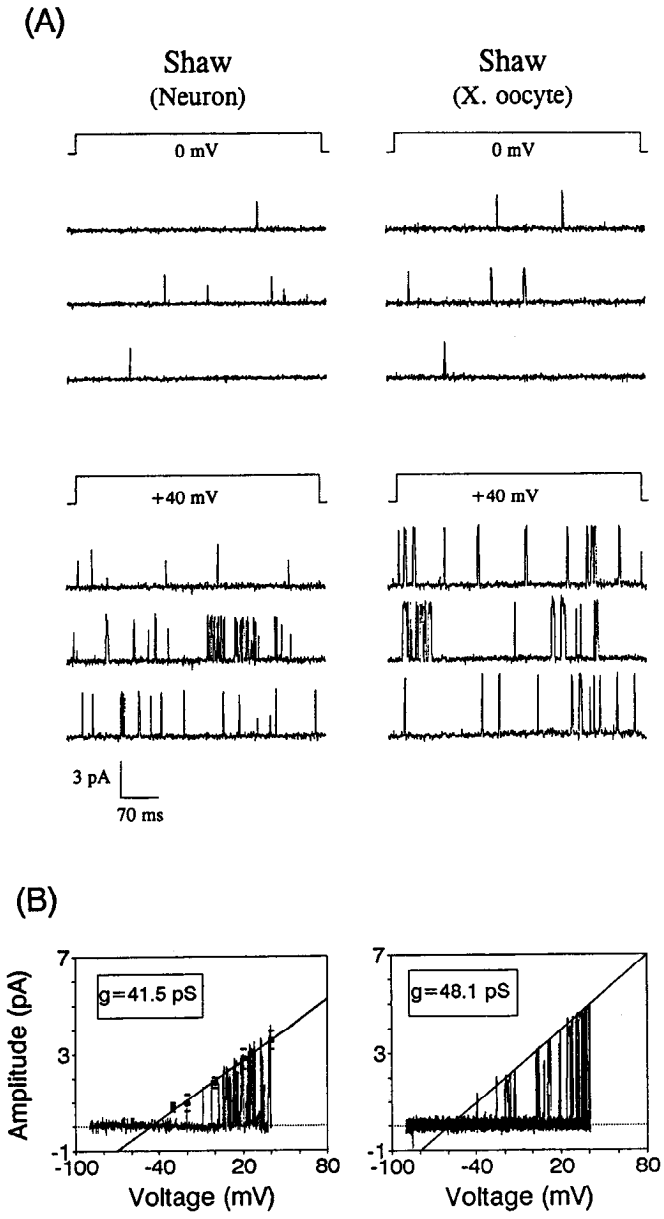

Figure 8. Shaw channels. *A,* Single-channel records of Shaw channel activity from embryonic *Drosophila* neurons (*left*) and *Xenopus* oocyte expression (*right*). Voltage jumps were preceded by a 500 msec prepulse to −60 mV to inactivate Shal channels. Patch from neuron contained two channels; oocyte patch contained one. Data were digitized at 0.488 msec/point and filtered at 2 kHz. *B,* Current versus voltage relation of single Shaw channels in embryonic *Drosophila* neurons (*left*) and in the *Xenopus* oocyte expression system (*right*). *Left,* Single record from a patch containing three channels while the voltage was ramped from −90 to +40 mV. Superimposed data points represent the average single-channel amplitude as determined by fitting a Gaussian distribution to amplitude histograms from multiple patches (N = 3–4). Standard deviations are as indicated. A line fit by linear regression to data points predicts a slope conductance of 41.5 pS. Data used for amplitude histograms was digitized at 0.195 msec/point and filtered at 2 kHz. *Right,* Shaw channel activity in a patch from *Xenopus* oocyte. Voltage was ramped from −90 to +40 mV. Due to the low open probability of a single Shaw channel in this patch, 19 records were superimposed. A line, fit by eye to the amplitudes of channel openings, predicts a slope conductance of 48.1 pS. All ramp records were digitized at 0.488 msec/point.

expressed in the late embryo along with *Shal* and *Shaw* (Fig. 11). Thus, in the absence of a deficiency for the *Shab* gene, several lines of evidence suggest that these slowly inactivating currents might be encoded by the *Shab* gene.

The largest and most common whole cell current component is the transient current removed by the *Shal* deficiency. As expected then, single Shal channels are the most frequently observed channels, appearing in 74% of patches. Although Shaw channels were observed in 54% of patches, their low open probability even at depolarized voltages (previously discussed) probably underlies the small, noninactivating component of whole cell current seen in some cells. Since Shaw channels have such a low voltage sensitivity, Shaw currents might function as "leak" currents. The correlation of the Shab-like channels to the whole cell slowly inactivating current component present in most cells is less certain since, as mentioned above, these channels tended to run down very rapidly. Thus, we cannot rule out the possibility that there may be yet another channel type present, perhaps in invaginations of the cell inaccessible to a patch pipette, that may be responsible for the slowly inactivating whole cell component.

Is Shaker present?

Consistent with previous reports (Solc et al., 1987; Saito and Wu, 1992), we find that *Shaker* is not responsible for a significant portion of the currents in the soma of neurons. Only 13% of the *Shal*-deficient neurons were observed to contain a transient component (Fig. 3). At most, *Shaker* could be responsible for this portion of transient current.

Northern analysis suggests that Shal, Shab, and Shaw genes are expressed in embryos

We investigated the developmental expression of the four cloned K^+ channel genes from *Drosophila* by Northern analysis (Fig. 11). PolyA-selected mRNA from early embryo, late embryo (the stage which most closely corresponds to the age of cells used in this study), pupa, and adult animal were run on an agarose gel under denaturing conditions, blotted onto nitrocellulose, and probed for each gene. Consistent with our physiological data, *Shal, Shab,* and *Shaw* appear to be prominently expressed in the late embryo, but *Shaker* expression is much weaker. Two alternatively spliced forms of both the *Shal* and *Shab* genes are expressed in the late embryo. Two forms of *Shal* have been cloned which differ in their 3′-carboxyl terminal ends (Baker, 1992). It is unlikely, however, that these two forms of *Shal* correspond to the two Shal gating modes described in this study, since both forms have been expressed and no differences noted in the whole-cell currents (Baker, 1992). *Shaw* appears to have only a single splice form throughout development. *Shaker* is expressed at very low levels in the late embryo, having its most prominent appearance in the pupal through adult stages.

Discussion

Shaker, Shal, Shab, and *Shaw* are the four genes encoding voltage-dependent K^+ channels currently cloned in *Drosophila* (Kamb et al., 1987; Papazian et al., 1987; Butler et al., 1989). The total voltage-dependent K^+ current in a given cell may consist of a mix of currents generated by these genes and perhaps other genes which have not yet been cloned. Each represents a separate subfamily of K^+ channel genes conserved across species. Each also constitutes an independent K^+ current system due to the fact that heteromultimers cannot form between them

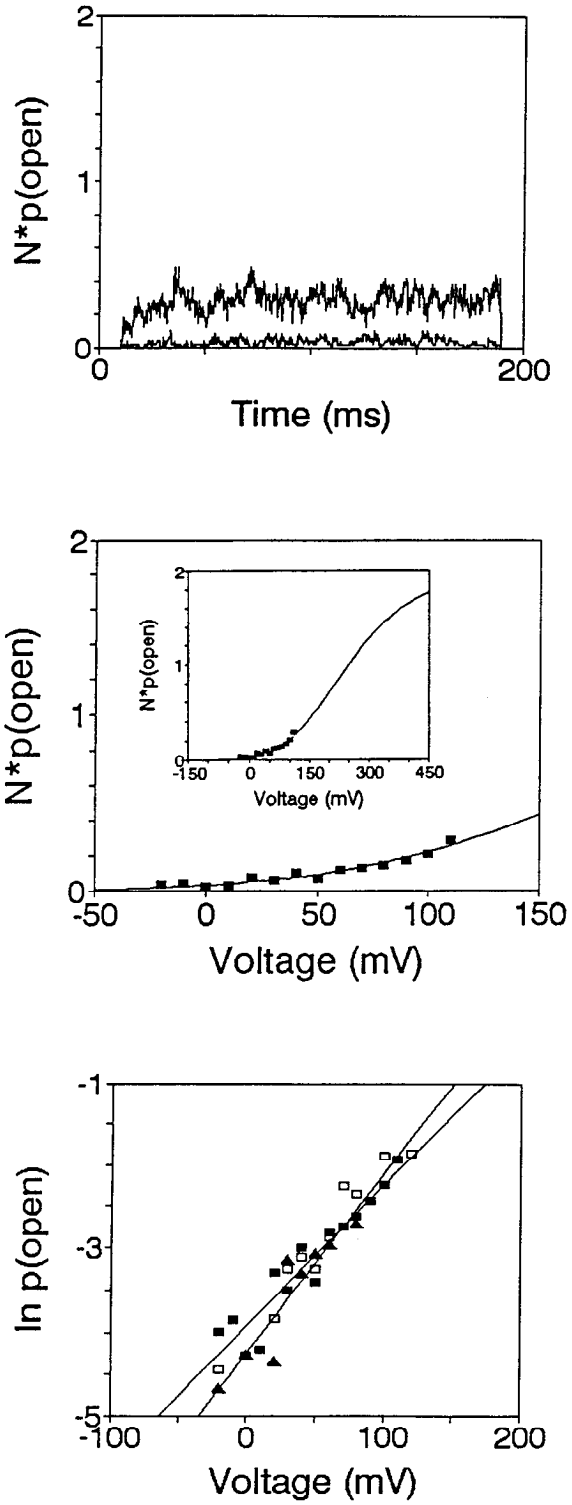

Figure 9. Shaw channels have an unusually low voltage sensitivity. *Top,* Ensemble averages of Shaw channel activity from embryonic neurons during voltage jumps (180 msec) to −20 mV and +110 mV. Holding potential was −60 mV. Average $N * p(\text{open})$, from 30 msec to 150 msec after jump onset, was 0.037 at −20 mV and 0.29 at +110 mV. N = total number of channels observed in patch; $p(\text{open})$ = probability of a channel being open. Patch contained two Shaw channels. Ensemble averages were constructed from 50 sweeps each. Data were digitized at 0.195 msec/point and filtered at 2 kHz. *Middle,* An example of $N * p(\text{open})$ for Shaw channels in a patch plotted versus membrane potential, where N = number of channels observed in the patch and $p(\text{open})$ = the probability of a single channel being open. $N * p(\text{open})$ values are determined from ensemble averages as described above from −20 mV to +110 mV, in 10 mV increments. Ensemble averages were constructed from 50 to 100 sweeps at each voltage. A Boltzmann equation to the fourth power, $N * p(\text{open}) = \max/[(1 + \exp[(V_{1/2} - V_m)/k])]$, was fit to data points. Since there appeared to be two channels present in this particular patch (although this may be an underestimate considering such a low open probability of channels), max was held at 2.0 while $V_{1/2}$ and k were varied. Best fits for parameters were $V_{1/2}$ = 65.38 mV and k = 110.70 mV/*e*-fold shift. This value for k corresponds to a single gate charge of 0.23 e^- and a total equivalent gating charge for opening a single Shaw channel of 0.92 e^- charges. *Inset* shows data points superimposed on extrapolated Boltzmann fit. *Bottom,* Semilogarithmic plot of $p(\text{open})$ versus membrane voltage from three patches containing Shaw channels (■, ▲, □). $N * p(\text{open})$ values were determined from ensemble-averaged currents as described in *A,* and normalized for the number of channels in each patch. The natural logarithm of each $p(\text{open})$ was then plotted versus membrane potential. Since these values correspond to very low open probabilities of the channel, they represent the linear portion of a single Boltzmann fit to such a semilogarithmic plot, the slope of which gives the "limiting logarithmic potential sensitivity" (Almers, 1978). Lines were fit through data points from each patch by linear regression. The total equivalent gating charge, Z, was calculated from the slopes of these lines by the relation $Z = (RT/F) * \ln[p(\text{open})/V_m]$. Values for Z from three patches were 0.43 e^-, 0.55 e^-, and 0.64 e^-, respectively.

(Covarrubias et al., 1991; Li et al., 1992; Sheng et al., 1993). Considerable diversity, however, can be achieved simply by mixing, in varying proportions, currents expressed by these independent K^+ current systems.

Diversity of K^+ currents within a single subfamily has also been observed to occur. In mammals, multiple genes within each subfamily may encode channels with related but variant properties (reviewed in Jan and Jan, 1990; Rudy et al., 1991; Salkoff et al., 1992). For example, Kv1.1 and Kv1.4 are both members of the *Shaker* subfamily but express currents that have very different inactivation rates (Stuhmer et al., 1989). In *Drosophila,* however, each subfamily appears to be represented by only a single gene. Both *Drosophila* and mammals generate additional diversity from some genes by alternative RNA splicing (Kamb et al., 1988; Pongs et al., 1988; Schwarz et al., 1988; Butler et al., 1989; Ghanshani et al., 1992). The *Shaker* gene in *Drosophila* is an extreme example, with as many as 24 alternatively spliced forms (Kamb et al., 1988). Heteromultimeric K^+ channels also contribute to K^+ current diversity. In mammals, heteromultimeric K^+ channels consisting of subunits from several distinct *Shaker* genes form *in vivo* (Sheng et al., 1993; Wang et al., 1993). In *Drosophila,* heteromultimeric channels may be formed by combining alternatively spliced forms from a single gene (Isacoff et al., 1990; McCormack et al., 1990). Finally, modulation such as phosphorylation can result in further K^+ current diversity (reviewed in Sieglebaum and Tsien, 1983; Levitan, 1985).

Sources of diversity

We found that embryonic *Drosophila* neurons display a wide variety of K^+ currents, consistent with previous reports (Byerly and Leung, 1988; Saito and Wu, 1991, 1992). We found that this variability is due to both a mix of currents from Shal, Shaw, and possibly Shab channels, and a variety of currents arising from Shal channels. The coexpression of *Shal, Shaw,* and *Shab* gives rise to a variety of whole-cell currents with different proportions of transient and steady-state components. A likely mechanism for Shal current diversity involves different gating modes, perhaps modulated by a mechanism such as phosphor-

←

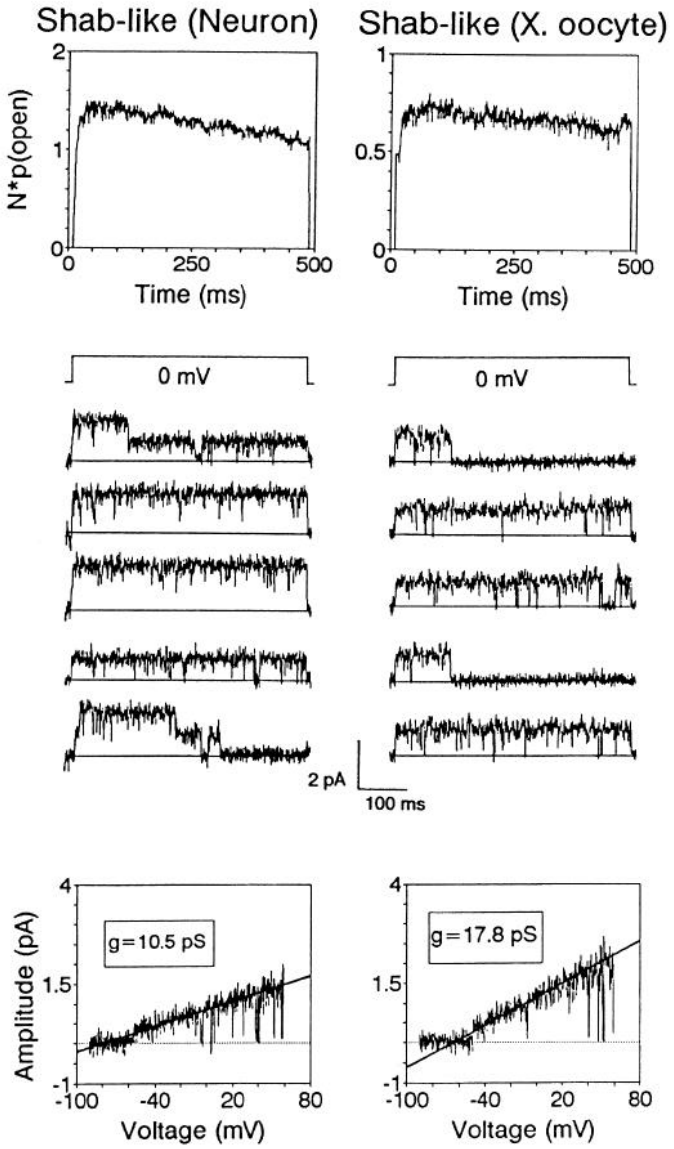

Figure 10. Shab-like channels in embryonic *Drosophila* neurons compared to Shab channels expressed in *Xenopus* oocytes. *Top,* Ensemble-averaged current from Shab-like channel activity in embryonic *Drosophila* neurons (*left*) and Shab channels as observed in the *Xenopus* oocyte expression system (*right*). Voltage jumps to 0 mV were preceded by a prepulse to −90 mV. Patch from embryonic neuron contained two channels, patch from *Xenopus* oocyte contained one. Ensemble averages were constructed from 49 (*left*) and 70 (*right*) sweeps. *Middle,* Representative single-channel records of Shab-like channels in embryonic *Drosophila* neurons (*left*) and Shab channels in the *Xenopus* oocyte expression system (*right*) used to construct ensemble-averaged currents above. *Bottom,* Single-channel current amplitude versus voltage relation of Shab-like channels in embryonic *Drosophila* neurons (*left*) and Shab channels as observed in the *Xenopus* oocyte expression system (*right*). The voltage was ramped from −90 to +60 mV. A line, fit by eye to the amplitudes of channel openings, predicts a slope conductance of 10.5 pS for the Shab-like channels in neurons (*left*), and 17.8 pS for Shab channels expressed in *Xenopus* oocytes (*right*). Data were digitized at 0.488 msec/point and filtered at 2 kHz.

ylation. Since single Shal channels appear, for the most part, to be in a fast or slow gating mode, various proportions of channels in each gating mode could give rise to macroscopic currents with inactivation time constants virtually spanning the entire range of inactivation rates seen.

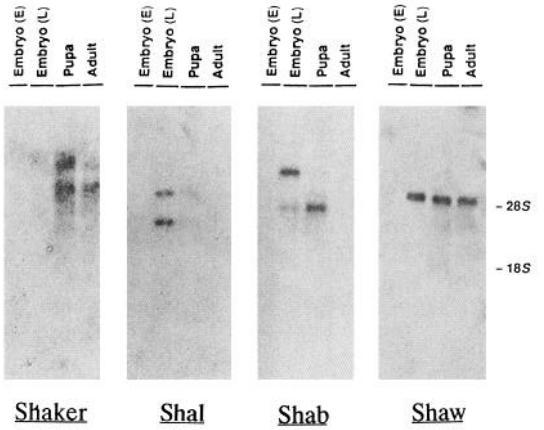

Figure 11. Northern analysis of *Shaker, Shal, Shab,* and *Shaw* at different stages of development. PolyA-selected mRNA (5 μg) was run on a denaturing agarose gel, blotted onto nitrocellulose, and probed with a ^{32}P-labeled cDNA probe for each of the four cloned *Drosophila* genes, as indicated. *Embryo (E),* Early embryo, 0–9 hr; *Embryo (L),* late embryo, 9–18 hr; *Pupa,* 4–5 d postpupariation; *Adult,* 1–2 weeks. Multiple bands in a lane probably correspond to alternatively spliced mRNAs.

Modal gating has also been previously described in other systems (Moorman et al., 1990; Alzheimer et al., 1993; Delcour et al., 1993). Modulation of ion channels has been reported to affect both the inactivation rates of currents (Numann et al., 1991; West et al., 1991; Zhou et al., 1991; Chabala et al., 1993; Kupper et al., 1993; Vyas et al., 1993; Drain et al., 1994; Rettig et al., 1994) and the gating mode of single channels (Yue et al., 1990; Zhou et al., 1991; Marrion, 1993; Wilson and Kaczmarek, 1993). A cloned skeletal muscle sodium channel, μI α-subunit, has been reported to have two gating modes which, like those of Shal, give rise to ensemble-averaged currents with very different rates of inactivation (Zhou et al., 1991). Phosphorylation has been suggested as a mechanism of modulation (Huganir et al., 1984; Levitan, 1985). Phosphorylation was reported to slow the inactivation rate of a mammalian Shaw channel (Vyas et al., 1993) and a rat brain Na^+ channel (Numann et al., 1991; West et al., 1991). Phosphorylation has also been reported to increase the inactivation rate of a Shaker K^+ current (Drain et al., 1994). A tyrosine phosphatase was reported to mediate the switch between gating modes in *Aplysia* bag cell cation channels (Wilson and Kaczmarek, 1993). Both phosphorylation and protein–protein interactions (Zhou et al., 1991) have been reported to modulate gating modes, and either may play a role in the regulation of Shal channel gating modes.

Shal is the most highly conserved of the four K^+ channel gene subfamilies with 82% amino acid identity between *Drosophila* and mouse (Pak et al., 1991). Such high conservation might indicate conservation in function with regard to modal gating behavior. Indeed, one report suggests that modulation of Shal channels in vertebrates also produces transient currents with different inactivation rates (Chabala et al., 1993).

The expression of Shal channels may not be restricted to embryonic neurons since their similarity to the A_2 channels in larval neurons (Solc et al., 1987, 1990; Solc and Aldrich, 1988) suggests that they too may be encoded by Shal. A_2 channels, like Shal channels, account for most of the transient currents present and give rise to ensemble-averaged currents with variable inactivation rates.

Low voltage sensitivity of Shaw channels

Our analysis of neuronal Shaw currents and a previous study of Shaw currents expressed in *Xenopus* oocytes both suggest an unusually low voltage sensitivity. The previous studies of macroscopic Shaw currents in the *Xenopus* oocyte expression system (Baker, 1992) were remarkably consistent with our results. The equivalent gating charge for a Shaw channel expressed in the oocyte system was determined by plotting tail current amplitudes versus prepulse potential. A Boltzmann equation to the fourth power was then used to fit the data, consistent with a model of four closed state transitions before opening (Zagotta and Aldrich, 1990). A total equivalent gating charge for opening a single Shaw channel was determined to be 0.86 e^- charges. This is in sharp contrast to the *Shaker* channel for which similar measurements predicted an equivalent gating charge of 7 e^- (Zagotta and Aldrich, 1990).

The fourth transmembrane segment (S4) of voltage-dependent K^+ channels is thought to be the "voltage sensor," containing a conserved structural motif of positively charged residues at every third position (Noda et al., 1984; Stuhmer et al., 1989; Liman and Hess, 1991; Papazian et al., 1991; Logothetis et al., 1992). With only four, Shaw has the lowest number of positively charged residues in its S4 region of all cloned K^+ channels (in contrast, Shaker contains seven). In addition to the low number of positive charges, the Shaw S4 region has two negatively charged residues in positions normally occupied by positively charged residues, bringing the net charge to +2 (Wei et al., 1989). This low net charge, compared with +7 for Shaker, perhaps underlies the low voltage sensitivity of Shaw channels.

As with *Shal, Shaw* gene expression may not be limited to embryonic neurons. The Shaw channels we observed resemble K_0 channels from cultured embryonic myotubes (Zagotta et al., 1988) and K_1 channels from larval neurons (Solc and Aldrich, 1988), which may all be products of the *Shaw* gene. These channels were also reported to have a large conductance (>40 pS). K_0 channels, like Shaw channels, displayed no apparent inactivation and a low open probability. K_0 and K_1 channels, like Shaw channels, most likely contribute a sustained outward whole-cell current, possibly serving the role of leak channels.

Of the three types of single-channel currents identified in embryonic neurons, only the 11 pS Shab-like channels gave rise to a slowly inactivating ensemble-averaged current. These channels are thus likely to produce the slowly inactivating currents observed in Shal-deficient neurons. Like Shal and Shaw channels, the expression of these Shab-like channels is also probably not restricted to embryonic neurons since their properties match those of K_D channels described in larval neurons (Solc and Aldrich, 1988) and embryonic myotubes (Zagotta et al., 1988), which may also be the products of the *Shab* gene. Both channels have a similar conductance (10–16 pS) and, once activated, both give rise to slowly inactivating ensemble-averaged currents.

Completeness of the "set"

To date, *Shaker, Shal, Shab,* and *Shaw* make up the "set" of voltage-dependent K^+ channel genes cloned in *Drosophila,* and represent the "set" of voltage-dependent K^+ channel gene subfamilies present in all metazoan organisms. However, the completeness of this "set" is currently unknown. We wanted to know whether we could assign all voltage-dependent K^+ currents in a given cell type to one of these four cloned genes. It should be noted, however, that K^+ channels expressed in the soma of the embryonic neurons used in this study are not necessarily representative of all K^+ channels expressed *in vivo.* There may be other K^+ channel genes expressed in particular subcellular locations, in other subpopulations of cells, or at different developmental stages. In addition, we cannot rule out the possibility that a different complement of channels might be expressed in cultured neurons than is expressed under normal conditions.

Previous mutant analysis of the *Shaker* gene showed it to be responsible for all of the voltage-dependent transient K^+ current in muscle of embryo, larvae, pupae, and adult (Salkoff and Wyman, 1981; Salkoff, 1983, 1985; Wu and Haugland, 1985; Solc et al., 1987; Zagotta et al., 1988; Broadie and Bate, 1993). In neurons, however, a *Shaker* mutation was found to have no perceptible effect on K^+ currents in larvae (Solc et al., 1987), and produced only a minor portion of transient K^+ currents in pupae (Baker and Salkoff, 1990). *Shaker* could be responsible for the 13% of transient currents remaining in *Shal*-deficient neurons. Previous reports have suggested that *Shaker* is expressed in the nerve terminals of the larval neuromuscular junction (Jan and Jan, 1977), in the adult cervical giant fiber axons (Tanouye and Ferrus, 1985), as well as in axons and neuropil of the adult *Drosophila* brain (Schwarz et al., 1990). It has also been reported that in the rat CNS, a *Shaker* ($K_v1.4$) gene's expression is more specific to axons and terminal regions, while a *Shal* ($K_v4.2$) gene's expression is more specific to the cell body and dendritic regions (Sheng et al., 1992). It is possible then that *Shaker* is expressed primarily in the axons and dendrites of neurons, thus remaining undetected by recording at the soma. Since all of the (voltage-dependent) single-channel currents observed in embryonic *Drosophila* neurons can be assigned to the remaining three cloned K^+ channel genes, then perhaps the "set" of known K^+ channel genes is nearing completion.

References

Almers W (1978) Gating currents and charge movements in excitable membranes. Rev Physiol Biochem Pharmacol 82:96–190.

Alzheimer C, Schwindt PC, Crill WE (1993) Modal gating of Na+ channels as a mechanism of persistent Na+ current in pyramidal neurons from rat and cat sensorimotor cortex. J Neurosci 13:660–673.

Baker K (1992) Diversity of K^+ currents expressed by a gene family conserved in *Drosophila* and mouse. PhD thesis, Washington University.

Baker K, Salkoff L (1990) The *Drosophila* Shaker gene codes for a distinctive K^+ current in a subset of neurons. Neuron 2:129–140.

Broadie KS, Bate M (1993) Development of larval muscle properties in the embryonic myotubes of *Drosophila melanogaster.* J Neurosci 13:167–180.

Butler A, Wei A, Baker K, Salkoff L (1989) A family of putative potassium channel genes in *Drosophila.* Science 243:943–947.

Byerly L, Leung HT (1988) Ionic currents of *Drosophila* neurons in embryonic cultures. J Neurosci 8:4379–4393.

Chabala LD, Bakry N, Covarrubias M (1993) Low molecular weight poly(A)+ mRNA species encode factors that modulate gating of a non-*Shaker* A-type K^+ channel. J Gen Physiol 102:713–728.

Covarrubias M, Wei A, Salkoff L (1991) *Shaker, Shal, Shab,* and *Shaw* express independent K^+ current systems. Neuron 7:763–773.

Delcour AH, Lipscombe D, Tsien RW (1993) Multiple modes of N-type calcium channel activity distinguished by differences in gating kinetics. J Neurosci 13:181–194.

Devore JL (1982) Probability and statistics for engineering and the sciences. Monterey, CA: Brooks/Cole.

Drain P, Dubin AE, Aldrich RW (1994) Regulation of *Shaker* K^+ channel inactivation gating by the cAMP-dependent protein kinase. Neuron 12:1097–1109.

Ghanshani S, Pak M, McPherson JD, Strong M, Dthlefs B, Wasmuth JJ, Salkoff L, Gutman GA, Chandy KG (1992) Genomic organiza-

tion, nucleotide sequence, and cellular distribution of a *Shaw*-related potassium channel gene, Kv3.3, and mapping of Kv3.3 and Kv3.4 to human chromosome 19 and 1. Genomics 12:190–196.

Gisselmann G, Sewing S, Madsen BW, Mallart A, Angant-Petit D, Muller-Holtkamp F, Ferrus A, Pongs O (1989) The interference of truncated with normal potassium channel subunits leads to abnormal behavior in transgenic *Drosophila melanogaster*. EMBO J 8:2359–2364.

Hardie RC (1991) Voltage-sensitive potassium channels in *Drosophila* photoreceptors. J Neurosci 11:3079–3095.

Hille B (1992) Ionic channels of excitable membranes. Sunderland, MA: Sinauer.

Huganir RL, Miles K, Greengard P (1984) Phosphorylation of the nicotinic acetylcholine receptor by an endogenous tyrosine-specific protein kinase. Proc Natl Acad Sci USA 81:6968–6972.

Isacoff EY, Jan Y-N, Jan LY (1990) Evidence for the formation of heteromultimeric potassium channels in *Xenopus* oocytes. Nature 345:530–534.

Jan LY, Jan Y-N (1982) Antibodies to horseradish peroxidase as specific neuronal markers in *Drosophila* and in grasshopper embryos. Proc Natl Acad Sci USA 79:2700–2704.

Jan LY, Jan Y-N (1990) How might the diversity of potassium channels be generated? Trends Neurosci 13:415–419.

Jan Y-N, Jan LY (1977) Two mutations of synaptic transmission in *Drosophila*. Proc R Soc Lond [Biol] 198:87–108.

Kamb A, Tseng-Crand J, Tanouye MA (1988) Multiple products of the *Drosophila Shaker* gene may contribute to potassium channel diversity. Neuron 1:421–430.

Kupper J, Marom S, Bowlby MR, Levitan IB (1993) Modulation of inactivation of the voltage-gated potassium channel Kv3. Soc Neurosci Abstr 294.15.

Levitan IB (1985) Topical review: phosphorylation of ion channels. J Membr Biol 87:177–190.

Li M, Jan Y-N, Jan LY (1992) Specification of subunit assembly by the hydrophilic amino-terminal domain of the *Shaker* potassium channel. Science 257:1225–1230.

Lichtinghagen R, Stocker M, Wittka R, Boheim G, Stuhmer W, Ferrus A, Pongs O (1990) Molecular basis of altered excitability in *Shaker* mutants of *Drosophila melanogaster*. EMBO J 9:4399–4407.

Liman ER, Hess P (1991) Voltage-sensing residues in the S4 Region of a mammalian K^+ channel. Nature 353:752–756.

Lindsley DL, Zimm GG (1992) The genome of *Drosophila melanogaster*. San Diego: Academic.

Logothetis DE, Movahedi S, Satler C, Lindpaintner K, Nadal-Ginard B (1992) Incremental reductions of positive charge within the S4 region of a voltage-gated K^+ channel result in corresponding decreases in gating charge. Neuron 8:531–540.

Marrion NV (1993) Selective reduction of one mode of M-channel gating by muscarine in sympathetic neurons. Neuron 11:77–84.

McCormack JW, Iverson LE, Rudy B (1990) Shaker K^+ channel subunits from heteromultimeric channels with novel functional properties. Biochem Biophys Res Commun 171:1361–1371.

Moorman JR, Kirsch GE, VanDongen AMJ, Joho RH, Brown AM (1990) Fast and slow gating of sodium channels encoded by a single mRNA. Neuron 4:243–252.

Noda M, Shimizu S, Tanabe T, Takai T, Kayano T, Ikeda T, Takahashi H, Nakayama H, Kanaoka Y, Minamino N, Kangawa K, Matsuo H, Raftery MA, Hirose T, Inayama S, Hayashida H, Miyata T, Numa S (1984) Primary structure of *Electrophorus electricus* sodium channel deduced from cDNA sequence. Nature 312:121–127.

Numann R, Catterall WA, Scheuer T (1991) Functional modulation of brain sodium channels by protein kinase C phosphorylation. Science 254:115–118.

Pak MD, Baker K, Covarrubias M, Butler A, Ratcliff A, Salkoff L (1991a) m*Shal*, a subfamily of A-type K^+ channel cloned from mammalian brain. Proc Natl Acad Sci USA 88:4386–4390.

Pak MD, Covarrubias M, Ratcliffe A, Salkoff L (1991b) A mouse brain homolog of the *Drosophila Shab* K^+ channel with conserved delayed-rectifier properties. J Neurosci 11:869–880.

Papazian DM, Schwarz TL, Tempel BL, Jan Y-N, Jan LY (1987) Cloning of genomic and complementary DNA from *Shaker*, a putative potassium channel gene from *Drosophila*. Science 237:749–753.

Papazian DM, Timpe LC, Jan Y-N, Jan LY (1991) Alteration of voltage-dependence of *Shaker* potassium channel by mutations in the S4 sequence. Nature 349:305–310.

Pongs O, Kecskemethy N, Muller R, Krah-Jentgens I, Baumann A, Kiltz HH, Canal I, Llamazares S, Ferrus A (1988) *Shaker* encodes a family of putative potassium channel proteins in the nervous system of *Drosophila*. EMBO J 7:1087–1096.

Rettig J, Heinemann SH, Wunder F, Lorra C, Parcej DN, Dolly JO, Pongs O (1994) Inactivation properties of voltage-gated K^+ channels altered by presence of β-subunit. Nature 369:289–294.

Reuter G, Szidonya J (1983) Cytogenetic analysis of variegation suppressors and a dominant temperature-sensitive lethal in region 23–26 of chromosome 2L in *Drosophila melanogaster*. Chromosoma 88: 277–285.

Rudy B (1988) Diversity and ubiquity of K^+ channels. Neuroscience 25:729–749.

Rudy B, Kentros C, Vega-Saenz de Miera E (1991) Families of potassium channel genes in mammals: toward an understanding of the molecular basis of potassium channel diversity. Mol Cell Neurosci 2: 89–102.

Saito M, Wu C-F (1991) Expression of ion channels and mutational effects in giant *Drosophila* neurons differentiated from cell division–arrested embryonic neuroblasts. J Neurosci 11:2135–2150.

Saito M, Wu C-F (1993) Ionic channels in cultured *Drosophila* neurons. EXS 63:366–389.

Salkoff L (1983a) *Drosophila* mutants reveal two components of fast outward current. Nature 302:249–251.

Salkoff L (1983b) Genetic and voltage-clamp analysis of a *Drosophila* K^+ channel. Cold Spring Harbor Symp Quant Biol 48:221–231.

Salkoff L (1985) Development of ion channels in the flight muscles of *Drosophila*. J Physiol (Lond) 80:275–282.

Salkoff L, Wyman R (1981) Genetic modification of potassium channels in *Drosophila Shaker* mutants. Nature 293:228–230.

Salkoff L, Baker K, Butler A, Covarrubias M, Pak MD, Wei A (1992) An essential "set" of K^+ channels conserved in flies, mice, and humans. Trends Neurosci 15:161–166.

Schwarz TL, Tempel BL, Papazian DM, Jan Y-N, Jan LY (1988) Multiple potassium-channel components are produced by alternative splicing at the *Shaker* locus in *Drosophila*. Nature 331:137–142.

Schwarz TL, Papazian DM, Carrettto RC, Jan Y-N, Jan LY (1990) Immunological characterization of K^+ channel components from the *Shaker* locus and differential distribution of splicing variants in *Drosophila*. Neuron 2:119–127.

Seecof RL, Donady JJ (1972) Factors affecting *Drosophila* neuron and myocyte differentiation *in vitro*. Mech Ageing Dev 1:165–174.

Seecof RL, Alleaume N, Teplitz RL, Gerson I (1971) Differentiation of neurons and myocytes in cell cultures made from *Drosophila* gastrulae. Exp Cell Res 69:161–173.

Seecof RL, Donady JJ, Teplitz RL (1973) Differentiation of *Drosophila* neuroblasts to form ganglion-like clusters of neurons *in vitro*. Cell Differ 2:143–149.

Sheng M, Tsaur M-L, Jan Y-N, Jan LY (1992) Subcellular segregation of two A-type K^+ channel proteins in rat central neurons. Neuron 9: 271–284.

Sheng M, Liao TJ, Jan Y-N, Jan LY (1993) Presynaptic A-current based on heteromultimeric K^+ channels detected *in vivo*. Nature 365: 72–79.

Shields G, Sang JH (1970) Characteristics of five cell types appearing during *in vitro* culture of embryonic material from *Drosophila melanogaster*. J Embryol Exp Morphol 23:53–69.

Siegelbaum SA, Tsien RW (1983) Modulation of gated ion channels as a mode of transmitter action. Trends Neurosci 6:307–313.

Singh S, Wu CW (1990) Properties of potassium currents and their role in membrane excitability in *Drosophila* larval muscle fibers. J Exp Biol 152:59–76.

Solc CK, Aldrich RW (1988) Voltage-gated potassium channels in larval CNS neurons of *Drosophila*. J Neurosci 8:2556–2570.

Solc CK, Aldrich RW (1990) Gating of single non-*Shaker* A-type potassium channels in larval *Drosophila* neurons. J Gen Physiol 96: 135–165.

Solc CK, Zagotta WN, Aldrich RW (1987) Single-channel and genetic analyses reveal two distinct A-type potassium channels in *Drosophila*. Science 236:1094–1098.

Stuhmer W, Conti F, Suzuki H, Wang X, Noda M, Yahagi N, Kubo H, Numa S (1989a) Structural parts involved in activation and inactivation of the sodium channel. Nature 339:597–603.

Stuhmer W, Ruppersberg JP, Schroter KH, Sakmann B, Stocker M, Giese KP, Perschke A, Baumann A, Pongs O (1989b) Molecular

basis of functional diversity of voltage-gated potassium channels in mammalian brain. EMBO J 8:3235–3244.

Szidonya J, Reuter G (1988) Cytogenetic analysis of the *echinoid* (*ed*), *dumpy* (*dp*) and *clot* (*cl*) region in *Drosophila melanogaster*. Genet Res 51:197–208.

Tanouye MA, Ferrus A (1985) Action potentials in normal and *Shaker* mutant *Drosophila*. J Neurogenet 2:253–271.

Vyas TB, Wei A, Salkoff L, Covarrubias M (1993) Fast inactivation of a human K^+ channel is regulated by protein phosphorylation. Soc Neurosci Abstr 294.17.

Wang H, Kunkel DD, Martin TM, Schwartzkroin PA, Tempel BL (1993) Heteromultimeric K^+ channels in terminal and juxtaparanodal regions of neurons. Nature 365:75–79.

Wei A, Covarrubias M, Butler A, Baker K, Pak M, Salkoff L (1990) K^+ current diversity is produced by an extended gene family conserved in *Drosophila* and mouse. Science 248:599–603.

West JW, Numann R, Murphy BJ, Scheuer T, Catterall WA (1991) A phosphorylation site in the Na^+ channel required for modulation by protein kinase C. Science 254:866–868.

Wilson GF, Kaczmarek LK (1993) Mode-switching of a voltage-gated cation channel is mediated by a protein kinase A–regulated tyrosine phosphatase. Nature 366:433–438.

Wu C-F, Haugland FN (1985) Voltage clamp analysis of membrane currents in larval muscle fibers of *Drosophila*: alteration of K currents in *Shaker* mutants. J Neurosci 5:2626–2640.

Yue DT, Herzig S, Marban E (1990) β-Adrenergic stimulation of calcium channels occurs by potentiation of high-activity gating modes. Proc Natl Acad Sci USA 87:753–757.

Zagotta WN, Aldrich RW (1990) Voltage-dependent gating of *Shaker* A-type potassium channels in *Drosophila* muscle. J Gen Physiol 95: 29–60.

Zagotta WN, Brainard MS, Aldrich RW (1988) Single-channel analysis of four distinct classes of potassium channels in *Drosophila* muscle. J Neurosci 8:4765–4779.

Zhong Y, Wu C-F (1991) Alteration of four identified K^+ currents in *Drosophila* muscle by mutations in *eag*. Science 252:1562–1564.

Zhou J, Potts JF, Trimmer JS, Agnew WS, Sigworth FJ (1991) Multiple gating modes and the effect of modulating factors on the μ1 sodium channel. Neuron 7:775–785.